



# HHS Public Access

Author manuscript

Cell Rep. Author manuscript; available in PMC 2024 July 15.

Published in final edited form as:

Cell Rep. 2024 June 25; 43(6): 114292. doi:10.1016/j.celrep.2024.114292.

## Commensal bacterial outer membrane protein A induces interleukin-22 production

Yanling Wang<sup>1</sup>, Vu L. Ngo<sup>1</sup>, Jun Zou<sup>1</sup>, Andrew T. Gewirtz<sup>1,2,\*</sup>

<sup>1</sup>Center for Inflammation, Immunity, & Infection, Institute for Biomedical Sciences, Georgia State University, Atlanta, GA 30303, USA

<sup>2</sup>Lead contact

### SUMMARY

Interleukin (IL)-22 promotes host-microbiota homeostasis. We sought to identify microbiota metabolite(s) that drive intestinal IL-22 production. We observed that exposing Peyer's patch cells (PPCs), *ex vivo*, to fecal supernatants (FSs) recapitulates fermentable fiber- and microbiota-dependent IL-22 production, and cellular sources thereof, thus supporting the use of this model. An interrogation of FSs generated from mice fed the fermentable fiber inulin (FS-Inu) revealed that its IL-22-inducing activity is mediated by heat-labile protein. Fractionation of FS-Inu by ion-exchange chromatography, and subsequent proteomic analysis of IL-22-inducing fractions, indicates that outer membrane protein A (OmpA) might be a microbial driver of IL-22 expression. Concomitantly, recombinant OmpA from *Parabacteroides goldsteinii*, which is enriched by an inulin diet, induces IL-22 production and expression of the IL-22-dependent genes REG3 $\gamma$  and  $\beta$ , in PPCs and mice. Thus, OmpA is one bacterial inducer of IL-22 expression, potentially linking diet, mucosal immune homeostasis, and gut health.

### Graphical abstract

---

This is an open access article under the CC BY-NC license (<http://creativecommons.org/licenses/by-nc/4.0/>).

\*Correspondence: [agewirtz@gsu.edu](mailto:agewirtz@gsu.edu).

#### AUTHOR CONTRIBUTIONS

Y.W., J.Z., and A.T.G. conceived the project and designed experiments. Y.W. and A.T.G. prepared the manuscript. Y.W. and V.L.N. performed the experiments and data analysis.

#### SUPPLEMENTAL INFORMATION

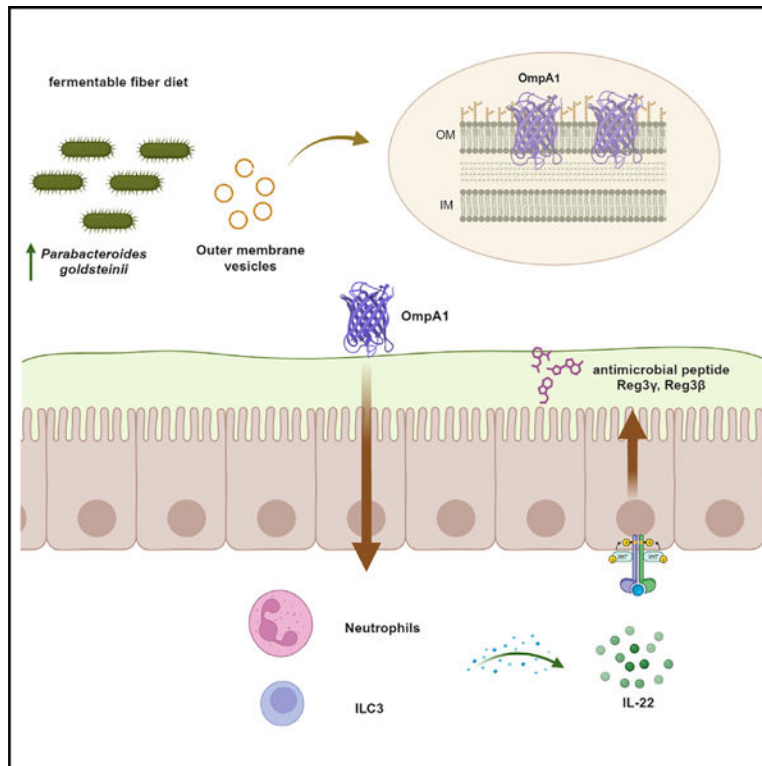
Supplemental information can be found online at <https://doi.org/10.1016/j.celrep.2024.114292>.

#### DECLARATION OF INTERESTS

The authors declare no competing interests.

#### ADDITIONAL RESOURCES

None.



## In brief

Wang et al. identify a microbiota-dependent activator of intestinal IL-22 production. Specifically, they show that *Parabacteroides goldsteinii*, a gut commensal that is enriched by a fermentable dietary fiber, induces IL-22 production in neutrophils and ILC3 via outer membrane protein A.

## INTRODUCTION

Proper management of gut microbiota by the mucosal immune system enables a stable, mutually beneficial host-microbiota relationship. An important mediator of this relationship is the cytokine interleukin (IL)-22.<sup>1</sup> IL-22 is homeostatically produced by intestinal lymphocytes in a manner that is largely dependent on gut microbiota and fermentable dietary fiber in that basal colonic IL-22 expression is markedly reduced in mice subjected to microbiota ablation and/or deprivation of fermentable dietary fiber.<sup>2</sup> IL-22 produced in the intestines of conventionally colonized fiber-fed mice drives epithelial proliferation, mucus production, and secretion of antimicrobial peptides, all of which work in concert to keep the inner mucus free of bacteria and, more generally, maintain a safe distance between the epithelium and gut bacteria. Lack of IL-22 production is implicated in the development of an array of chronic inflammatory disease states including metabolic syndrome and inflammatory bowel disease.<sup>3</sup> Mechanism(s) by which nourishing microbiota with fermentable dietary fiber elicit IL-22 production have not been fully defined. Some microbiota-derived molecules, including flagellin, short-chain fatty acids (SCFA), indole derivatives, and n-formylated peptides, are capable of inducing IL-22 production in some contexts,<sup>4-6</sup> but efforts to link these molecules to homeostatic fiber-mediated IL-22

production argued against their involvement.<sup>2</sup> For example, neither genetic ablation of Toll-like receptor 5 (TLR5) nor blockade or SCFA generation reduced IL-22 expression in fiber-fed mice,<sup>2</sup> thus suggesting that other microbial inducers of IL-22 await identification. We herein report one step toward filling this gap of knowledge. Specifically, we report that an outer membrane protein A (OmpA) protein, herein termed OmpA1, from gut commensal *Parabacteroides goldsteinii* activates intestinal IL-22 expression, potentially playing a role in linking fermentable fiber to gut health.

## RESULTS

### ***Ex vivo* assay of PPCs recapitulates fermentable fiber- and microbiota-dependent induction of IL-22**

The ablation of microbiota or the deprivation of fermentable dietary fiber markedly reduces intestinal expression of IL-22.<sup>2</sup> We hypothesize that this reflects that fiber-nourished gut bacteria produce a metabolite(s) that drives IL-22 production. Hence, we sought to develop an *ex vivo* model that would allow us to identify fermentable-fiber- and microbiota-dependent molecules capable of activating IL-22 production. Fecal supernatants (FSs) of mice fed compositionally defined diets containing only insoluble fiber, cellulose, or a soluble/fermentable fiber, inulin, were applied to freshly isolated preparations of murine Peyer's patch cells (PPCs; Figure 1A), mesenteric lymph node cells, and lamina propria (LP) cells. PPCs, but not the other cell preparations, reliably displayed production of IL-22 in response to FSs generated from mice fed diets containing inulin (FS-Inu) (Figures 1B and S1). PPC IL-22 production was dependent on fermentable fiber in that PPCs did not produce statistically significant levels of IL-22 in response to FSs from mice fed the cellulose-enriched diet (FS-Cel). The ability of FS-Inu to induce IL-22 by PPCs was ablated by administering mice antibiotics and was not present in FSs from germfree mice consuming a fiber-rich, grain-based chow diet (Figure 1B). Exposure of PPCs to PBS or FS-Inu *ex vivo*, and subsequent analysis by flow cytometry, revealed that FS-Inu increased the levels of IL-22<sup>+</sup> neutrophils and type 3 innate lymphoid cells (ILC3s) (Figures 1C–1H). Such increases were seen in relative and absolute numbers of IL-22<sup>+</sup> cells despite FS-Inu modestly reducing the number of live cells (total live cells post-stimulation for PBS and FS-Inu were  $(197 \pm 7) \times 10^3$  vs.  $(150 \pm 9) \times 10^3$ , respectively). A similar cellular pattern of IL-22<sup>+</sup> cells was observed in freshly isolated PPCs from mice fed diets that contained only cellulose or inulin as a fiber source (Figure 1I). Freshly isolated colonic and ileal LP cells from inulin-fed mice also exhibited significantly higher IL-22<sup>+</sup> neutrophils and ILC3s than those from cellulose-fed mice. The notion that ILC3s and neutrophils are the predominant producers of IL-22 accords with previous work.<sup>7</sup> Collectively, these results indicate that the microbial dependence, dietary determinants, and cellular sources of IL-22 expression *in vivo* resemble what we, herein, observed in PPCs exposed to FSs, thus supporting the use of this *ex vivo* model as a platform to seek the identities of microbial-derived IL-22-inducing metabolites.<sup>2</sup>

### **Characterization of the IL-22-inducing activity of FS-Inu suggests heat-sensitive protein(s)**

We next sought to identify the molecule(s) present in FS-Inu that drove IL-22 production in our *ex vivo* model. We first considered potential roles for previously reported microbial

inducers of IL-22. In contrast to the case of FS-Inu, PPCs did not generate detectable levels of IL-22 in response to SCFAs, lipopolysaccharide, or the canonical n-formylated peptide, N-formyl-L-methionyl-L-leucyl-L-phenylalanine (fMLF) (Figure S2A). In accord with earlier work, purified bacterial flagellin potently induced IL-22 from PPCs (Figure S2B).<sup>5</sup> In further accord with such studies, flagellin's ability to activate IL-22 expression withstood 100°C<sup>8</sup> and was neutralized by an anti-IL-23 antibody.<sup>5</sup> However, in contrast to flagellin, FS-Inu's ability to induce IL-22 from PPCs was destroyed by heating to 100°C and was not impacted by IL-23 neutralization. Further assessment of its heat stability found that the ability of FS-Inu to induce IL-22 in this system withstood 50°C but was markedly reduced by 65°C, suggesting the involvement of a heat-denaturable protein (Figure 2A). In accord with this notion, exposure of FS-Inu to proteinase K-linked agarose beads markedly lowered its IL-22-inducing activity (Figure 2B). Thus, we hypothesized that FSs from inulin-fed mice contained a protein capable of activating IL-22 from PPCs and sought to identify it.

### **Purification and proteomic analysis yields OmpA as a candidate driver of FS-Inu's IL-22-inducing capacity**

We sought to purify IL-22-inducing protein(s) present in FS-Inu by ion-exchange chromatography and observed that the IL-22-inducing factor bound negatively charged, but not positively charged, resins (Figure 2C). Hence, FS-Inu was applied to an anion-exchange column, which was then subjected to increasing NaCl concentrations. While most fractions exhibiting significant IL-22-inducing activity contained numerous proteins, we observed a 34 kDa band whose abundance positively associated with IL-22-inducing bioactivity (Figure 2D). We next sought to reduce the complexity of our model by using mice with a limited defined microbiota, namely gnotobiotic mice carrying only the 8-member collection of bacteria known as the Altered Schaedler Flora (ASF).<sup>9</sup> FS-Inu from ASF mice indeed induced IL-22 from PPCs (Figure 2E). Subjecting ASF FS-Inu to anion-exchange chromatography found most of the IL-22-inducing bioactivity eluted in fractions that contained a relatively prominent band with an apparent molecular weight of 34 kDa (Figure 2F). The 34 kDa bands obtained from FS-Inu of conventional and ASF mice were excised and subjected to mass-spectrometry-based proteomic analysis. The band from ASF FS-Inu yielded 2 prominent candidates, one of which, namely OmpA, consistent with its expected molecular weight (Figure 2G), was present in the ASF genome and, furthermore, was also the most prominent candidate attained from proteomic analysis of conventional FS-Inu (Figure 2H). These results led us to hypothesize that OmpA may be a fermentable-fiber-induced protein capable of potentiating IL-22 expression.

### **Membrane and OMVs of *P. goldsteinii* strain ASF519 induced IL-22 in PPC**

OmpA is an abundant transmembrane protein found in an array of gram-negative bacteria. Its presence in FS-Inu could result from the abundant secretion of vesicles increasingly appreciated to mediate microbiota influences on its host.<sup>10</sup> In accord with this hypothesis, we found that membrane vesicles isolated from FS-Inu by ultracentrifugation were indeed enriched in IL-22-inducing bioactivity, while the removal of such vesicles significantly reduced the ability of FS-Inu to induce IL-22 (Figure 3A). Analyses of microbiomes from ASF mice via 16s rRNA sequencing found that strain ASF519, which belongs to

species *P. goldsteinii*, was enriched in mice fed an inulin-enriched diet, encompassing about 70% of reads (Figure 3B). Furthermore, qPCR confirmed that the abundance of *P. goldsteinii* was increased by enriching the diet with inulin in ASF mice (Figure S3). Genus *Parabacteroides* are gram-negative, obligate anaerobic, non-motile rods.<sup>11</sup> They are common commensals in human intestines, comprising about 3.5% of the microbiota of Americans, and were estimated to be present in approximately 90% of individuals.<sup>12</sup> Thus, we chose *P. goldsteinii* to investigate the notion that OmpA promotes IL-22 production. We found that preparations of membrane and secreted outer membrane vesicle (OMV) of pure cultures of *P. goldsteinii* strain ASF519 indeed contained a proteinase K-sensitive, heat-denaturable, and IL-23-independent activator of PPC IL-22 expression (Figures 3C and 3D), which is in accordance with the IL-22-inducing factor in FS-Inu.

### A recombinant *P. goldsteinii* OmpA induces IL-22 in PPC and *in vivo*

Investigation of the genome of *P. goldsteinii* strain ASF519 revealed the existence of 7 different *OmpA* genes, which we refer to herein as OmpA 1–7 based on the order of their positions in the genome. Based on how well they matched the proteomic analysis prediction scores, we selected OmpA 1, 3, 4, and 5 for further study, attempting to generate recombinant versions of each protein. We also sought to generate OmpA from *Salmonella typhimurium*, as this OmpA closely matched the proteomic analysis, although this may reflect that the protein database used for such analysis is biased toward well-characterized bacteria. In accordance with previous experiences of others, transmembrane proteins are difficult to express in high abundance, resulting in a high background in the recombinant protein during purification. To overcome this hurdle, we incorporated an expression control (denoted as “–”), wherein the background protein was purified from the same expression strain cultures, but the promoter was not induced with Isopropyl  $\beta$ -D-thiogalactopyranoside (IPTG) (Figure 4A). Lack of recombinant His-tagged OmpA in the expression control was confirmed by SDS-PAGE and western blot against a His tag (Figures 4B, S4A, and S4B). Initial screening of these candidates found that only *P. goldsteinii* OmpA1 consistently induced IL-22 production relative to cognate expression controls (Figures S4C and S4D). OmpA from *S. typhimurium* did not induce IL-22 from PPCs, despite a high matching score of proteomic analysis (Figures S4C and S4D). Further investigation found that OmpA1 consistently induced IL-22 expression in PPCs (Figure 4C). Reminiscent of our earlier findings with FS-Inu, PPCs administered OmpA1 displayed IL-22<sup>+</sup> neutrophils and, to a lesser extent, ILC3s (Figures 4D–4I), but in contrast to FS-Inu, OmpA1 did not impact PPC viability (total live cells post-stimulation for PBS, expression control, and OmpA1 were  $(541 \pm 17) \times 10^3$  vs.  $(551 \pm 16) \times 10^3$  vs.  $(537 \pm 18) \times 10^3$ , respectively).

We next considered the extent to which OmpA1 might be a physiologically significant driver of IL-22 *in vivo*. First, we investigated the potential of OmpA1 to induce functionally relevant levels of IL-22 *in vivo*. We found that intraperitoneal administration of OmpA1, but not expression control, increased serum IL-22 concentrations (Figure 4J) and ileal expression of antimicrobial peptides Reg3 $\gamma$  and Reg3 $\beta$  (Figure 4L), both of which are known to be key downstream mediators of IL-22's biological impacts. We next probed if the elevated IL-22 expression that results from enriching the diet with inulin might associate with increased OmpA1 expression. This was indeed the case as, relative to non-fermentable

fiber cellulose, mice fed inulin-enriched diets displayed higher copies of *ompA1* genes in ASF mice (Figure S3). Collectively, these results accord with the notion that OmpA1 contributes to the increased IL-22 expression upon consumption of fermentable dietary fibers such as inulin.

## DISCUSSION

IL-22 is appreciated to play a central role in maintaining a healthy intestinal mucosa. IL-22 is produced by intestinal lymphocytes and acts, via the IL-22 receptor, which is primarily expressed by gut epithelial cells, to drive enterocyte proliferation, secretion of mucus, and release of antimicrobial peptides. Together, such actions of IL-22 help protect the host from the vast diverse microbial ecosystem that inhabits the intestinal tract. Accordingly, IL-22 expression is regulated by gut microbiota in that reducing gut bacterial mass by gnotobiotic approaches or deprivation of dietary fiber lowers IL-22 expression.<sup>2</sup> Yet, how gut bacteria, and/or their metabolites, maintain gut IL-22 expression in fiber-fed mice has remained largely unknown. We herein report one step toward filling this gap of knowledge. Specifically, we report that gut commensal *P. goldsteinii* OmpA1 is one microbial product that can activate IL-22 expression *in vitro* and *in vivo* and contributes to the intestinal IL-22 expression that is driven by consumption of fermentable dietary fiber.

The notion that OmpA1 drives IL-22 production was yielded by our *ex vivo* model, wherein we measured the ability of FSs, and subsequently fractions thereof, to elicit IL-22 production from PPCs. That such IL-22 production in response to both the starting FS-Inu and recombinant OmpA1 associated with the appearance of both IL-22<sup>+</sup> neutrophils and ILC3s strongly suggests that it was mediated by both cell types. Furthermore, that this cellular pattern of IL-22 expression was like that observed in inulin-fed mice supports the physiological relevance of this model. In contrast to PPCs, LP cells did not produce IL-22 when exposed to FS-Inu *ex vivo*, even though such cells became positive for IL-22 *in vivo* in response to feeding mice an inulin-enriched diet. We speculate that such a failure of LP cells to produce IL-22 *ex vivo* may reflect their low viability in cell culture. Consequently, we view our findings as indicating that PPCs served as a viable *ex vivo* model that produced a candidate IL-22 inducer, namely OmpA, which was validated *in vivo*, but do not speak to the relative roles of PPCs vs. LP cells in producing IL-22 *in vivo*. The role of ILC3s in mediating intestinal IL-22 production accords with numerous studies,<sup>3</sup> as well as our observation that inulin-induced IL-22 production was markedly reduced in *Rag2<sup>-/-</sup>IL2rg<sup>-/-</sup>* mice, which lack all T cells and B cells as well as ILC3s.<sup>2</sup> The appearance of IL-22<sup>+</sup> neutrophils in our models was less anticipated but accords with the report that colonic neutrophils are also capable of producing IL-22.<sup>7</sup> Like the IL-22 produced by ILC3s, the IL-22 produced by neutrophils promotes epithelial integrity and drives expression of antimicrobial peptides such as Reg3 $\beta$ .<sup>7</sup> Relating the relative abundance of cells that contain IL-22, or any other intracellular cytokine, measured by flow cytometry, to the relative role of that cell type in determining levels of the secreted bioactive cytokine or its effectors, in the case of IL-22 assessed by ELISA and Reg3 $\gamma$ / $-\beta$  expression, respectively, is not straight forward. Thus, we do not view our results as speaking to the relative importance neutrophils or ILC3s in mediating inulin-induced IL-22 production but simply conclude that both cell types contribute in our PPC model and *in vivo*.

OMPAs are an essential class of the outer membrane of gram-negative bacteria. OmpA, one of the best-characterized OMPs, is notably abundant, with an estimated presence of around 10,000 copies per cell in some bacteria.<sup>13</sup> OmpA's structural features are best characterized in *E. coli*, revealing an eight-stranded beta-barrel configuration. OmpAs from gram-negative bacterial pathogens such as *S. typhimurium*, *Klebsiella pneumoniae*, *Pseudomonas aeruginosa*, and *Acinetobacter baumannii*, have also been extensively investigated in terms of both structure and their role in infection. These studies have unveiled the versatile function of OmpAs: acting as integral membrane components, participating in ion transport, serving as receptors for bacteriophages, and contributing to pathogenesis.<sup>14,15</sup> OMPs in general, and OmpAs in particular, are also common in commensal bacteria but have not been extensively studied. Commensurate with the idea that they are germane to bacterial metabolism, OmpAs have long been thought to be highly conserved, but more recent studies have challenged this belief.<sup>16</sup> Indeed, a sequence analysis of OmpAs from an array of pathogenic and commensal microbes reveals both highly conserved and highly diverse regions, although, by themselves, these features do not explain why only some OmpAs activated IL-22 (Figures S4C and S4D). Overall sequence similarity among OmpAs from various bacteria species varies greatly from 16% to 97% (Figure S5). *P. goldsteinii* OmpA1 shares its greatest similarity with *P. aeruginosa* (52%). However, even within the same bacterial species or strain, OmpAs display considerable diversity, as the sequence similarity among the seven OmpAs of *P. goldsteinii* also varies greatly from 16% to 90% (Figure S5). These variations highlight the need for future studies to define epitopes by which OmpA1 drives IL-22 production and, subsequently, unravel their unique and shared properties and functions of OmpA proteins.

The notion that OmpA might be recognized by the host to promote IL-22 expression fits with earlier findings that OmpA can serve as a microbial-associated molecular pattern capable of activating innate immunity. For instance, OmpAs from *K. pneumoniae* can activate dendritic cells (DCs), natural killer cells, and macrophages via TLR2, leading to rapid release of defensins causing a disruption of the bacterial membrane.<sup>17</sup> In addition, OmpAs from enterohemorrhagic *E. coli* and *A. baumannii* have been reported to induce DCs to secrete cytokines such as IL-1, IL-10, and IL-12.<sup>18,19</sup> Our findings herein support this general paradigm but suggest that it may well apply to commensal microbes as well. How OmpAs from non-invasive commensal microbes such as *P. goldsteinii* might reach mucosal immune cells is not yet clear, but we note that OmpAs are secreted in OMVs.<sup>20</sup> That the strong IL-22-inducing activity, shown by OMVs in FS-Inu (Figure 3A) and of pure culture of *P. Goldsteinii* strain ASF519 (Figure 3D), may explain how commensal bacteria stimulate host immune responses despite remaining in the outer regions of the mucus layer. We speculate that a better understanding the potential of OmpA1 in OMVs to drive IL-22 production may enable future therapeutic strategies wherein increased IL-22 production might be desirable.

### Limitations of the study

The major limitation in our findings is that we do not know if OmpA-induced IL-22 is a major contributor to the overall levels of gut IL-22 expression in conventional fiber-fed mice. It is certainly possible that its role is modest or even insignificant. For example,

both flagellin and SCFAs can drive IL-22 expression in some contexts, but neither ablation of TLR5 signaling nor SCFA generation *in vivo* lowers intestinal expression of IL-22 in fiber-fed mice.<sup>2</sup> Unfortunately, we do not yet have the means of specifically eliminating OmpA-induced IL-22 and thus cannot rule out the possibility that this pathway is simply one of many means of inducing this important cytokine. We hope that, in the future, we will overcome this hurdle by generating OmpA-deficient *P. goldsteinii* mutants and/or identifying an OmpA receptor, but efforts toward this goal have been stymied by the difficulty in generating targeted mutations in commensal slow-growing anaerobes such as *P. goldsteinii*. Another technical limitation is our current inability to generate large quantities of highly pure OmpAs, likely reflecting inherent difficulties in the large-scale purification of recombinant membrane proteins. Nonetheless, we report a step toward better understanding of gut IL-22 expression, namely that OmpA from gut commensal *Parabacteroides* is one common bacterial molecule capable of activating gut IL-22 expression.

## STAR★METHODS

### RESOURCES AVAILABILITY

**Lead contact**—Further information and requests for resources and reagents should be directed to and will be fulfilled by the lead contact, Andrew Gewirtz (agewirtz@gsu.edu).

**Materials availability**—Plasmids generated in this study will be shared upon reasonable request from the lead contact.

#### Data and code availability

- The raw 16s rRNA sequencing data have been deposited at NCBI SRA: PRJNA1089129. The processed proteomics data has been deposited at Georgia State University institutional repository (<https://doi.org/10.57709/VK8T-YA18>).
- This paper does not report original code.
- Any additional information required to reanalyze the data reported in this work paper is available from the lead contact upon request.

### EXPERIMENTAL MODEL AND STUDY PARTICIPANT DETAILS

**Mice and diet**—8-week-old female C57BL/6 mice were purchased from Jackson Labs (Bar Harbor, ME) and maintained at Georgia State University via procedures approved by its institutional animal use and care committee under protocol #s A17047 and A24001. Mice were fed compositionally defined diets enriched with inulin or cellulose (herein referred as inulin or cellulose diets, Research Diets, Inc.) for 4–6 weeks. Feces were collected daily starting from one week on diet and stored at –80°C for later analysis. Antibiotics, when indicated, containing vancomycin (0.5 g/L), neomycin (1 g/L), metronidazole (1 g/L) and ampicillin (1 g/L) was given to mice in drinking water for 2 weeks while mice were remained on inulin diet. Feces were collected starting from one week following antibiotic treatment and stored at –80°C for later analysis.

Altered Schaedler Flora (ASF) mice were generated by inoculating C57BL/6 germ-free mice with ASF feces (ASF Taconic Inc. Hudson, NY) in drinking water which contained 8 ASF strains.<sup>21</sup> Such ASF mice were bred and maintained in isolators at Georgia State University. Mice were fed irradiated compositionally defined diets enriched with inulin or cellulose (Research Diet, Inc.) for 2–4 weeks, and feces were collected and stored at  $-80^{\circ}\text{C}$  for later analysis.

**Peyer's patch cell *ex vivo* model**—12-week-old female C57BL/6 mice were purchased from Jackson Labs (Bar Harbor, ME) and maintained on a standard grain-based chow diet. During sacrifice, Peyer's patch cells (PPC) from small intestine were collected. After homogenization, PPC were pass through 70  $\mu\text{m}$  strainer and were cultured in RPMI media supplemented with 10% FBS, penicillin-streptomycin, L-glutamine and at density of  $10^6$  cells/200  $\mu\text{L}$ . Various stimulants were added in PPC at different concentrations and incubated for 16 h.

**Bacteria strain and culture condition**—*P. goldsteinii* strain ASF519 were cultured in brain heart infusion (BHI) medium at  $37^{\circ}\text{C}$  in anaerobic condition. *E. Coli* BL21 strain for recombinant protein purification was cultured in LB medium supplemented with antibiotics (carbenicillin, Sigma) at  $37^{\circ}\text{C}$  with shaking rpm = 200.

## METHOD DETAILS

**Preparation of fecal supernatant (FS) and its vesicles**—Feces were collected according to the above methods and were resuspended in PBS as 100 mg/mL and vortexed extensively until no visible pellet was seen, prior to centrifugation ( $21,000 \times g$  for 10min with the exception of 40 min for inulin feces). Supernatant (FS) was stored at  $-80^{\circ}\text{C}$ .

For vesicle preparation, FS was further ultra-centrifuged at  $110,000 \times g$  at  $4^{\circ}\text{C}$  or 2 h. The pellet (vesicles) was suspended and sonicated briefly in PBS.

**ELISA**—For *ex vivo* assays, following 16h of incubation, media of PPC culture was taken and IL-22 production was measured by DuoSet Mouse IL-22 ELISA kit (R&D) according to the manufacture's protocol. For serum IL-22, retro orbital blood was taken from mice administered recombinant protein OmpA. Serum was prepared from blood by centrifugation at  $2,000 \times g$  for 10min. IL-22 in the serum was quantified by Mouse/Rat IL-22 Quantikine ELISA Kit (R&D) according to the manufacture's protocol.

**Ion-exchange chromatography and proteomic sequencing**—Fecal supernatant (FS) from ASF mice or conventional mice fed with inulin diet, was purified using ion-exchange chromatography (Uno q1, Bio-rad column, coupled with Duo-flow LC system). Briefly, FS was diluted with distilled water to reduce ion strength in the sample and then loaded to the column. After extensive washing, proteins were eluted with gradient salt (up to 1M NaCl) and fractions of each 0.5mL eluate were collected. Protein abundance was monitored by UV detector at 280nm. Each fraction was desalted and concentrated using 10k Amicon filter (Millipore). IL-22 induction activity of each fraction was assessed by PPC model.

Fractions able to induce IL-22 production were further separated by SDS-PAGE gels and visualized by Commassie blue staining. Suspected bands were cut out from SDS-PAGE gels and submitted for proteomic sequencing (Creative protein, NJ, USA). Briefly, the protein band samples were digested by trypsin, and identified by nano LC-MS/MS. Digested peptides were resuspended in 0.1% formic acid and 1 µg sample was loaded to Ultimate 3000 nano UHPLC system coupled with a Q Exactive HF mass spectrometer with an ESI nanospray source (ThermoFisher Scientific, USA), at a flow rate of 250 nL/min. Mobile phase A: 0.1% formic acid in water; B: 0.1% formic acid in 80% acetonitrile. LC linear gradient: from 2 to 8% buffer B in 3 min, from 8% to 20% buffer B in 40 min, from 20% to 40% buffer B in 28 min, then from 40% to 90% buffer B in 4 min. For mass spectrometry, the full scan was performed between 300 and 1,650 m/z at the resolution 60,000 at 200 m/z, the automatic gain control target for the full scan was set to 3e6. The MS/MS scan was operated in Top 20 mode using the following settings: resolution 15,000 at 200 m/z; automatic gain control target 1e5; maximum injection time 19ms; normalized collision energy at 28%; isolation window of 1.4 Th; charge state exclusion: unassigned, 1, >6; dynamic exclusion 30 s. The raw MS files were analyzed and searched against bacteria protein database using Maxquant (1.6.2.6). The parameters were set as follows: the protein modifications were carbamidomethylation (C)(fixed), oxidation (M) (variable); the enzyme specificity was set to trypsin; the precursor ion mass tolerance was set to 10 ppm, and MS/MS tolerance was 0.5 Da.

**16s rRNA gene sequencing**—Fecal DNA of ASF mice fed with either cellulose diet or inulin diet was extracted using DNeasy 96 PowerSoil Pro QIAcube HT Kit (Qiagen) and the region V3-V4 of 16S rRNA genes were amplified using the following primers: 341F 5'TCGTCGGCAGCGTCAGATGTGTATAAGAGACAGCCTACGGGNGGCWGCAG-3'; 805R 5'GTCTCGTGGGCTCGGAGATGTGTATAAGAGACAGGACTACHVGGGTATCTAATC C-3'. PCR products of each sample were purified using Ampure XP magnetic purification beads. An index PCR was performed to attach dual barcodes and Illumina sequencing adapters using Nextera XT Index kit (Illumina). Final PCR products was verified on 1.5% DNA agarose gel and quantified using Pico dsDNA assay (Invitrogen). An equal molar of each sample was combined and purified again using Ampure XP beads as the library. The library was diluted and spiked with 10% PhiX control (Illumina) and sequenced by Illumina iSeq 100 Sequencing System (2 × 150bp). Demultiplexed fastq files were generated on instrument. Demultiplexed fastq files were generated on instrument. Sequence reads were quality filtered by DADA2 plugin in Qiime2.<sup>22</sup> Taxonomy was assigned based on the Greengenes database.

***P. goldsteinii* membrane and OMV purification**—Membrane fractions were purified from *P. goldsteinii* strain ASF519 culture using a method described before.<sup>23</sup> Briefly, cells were pelleted from 0.5L culture and lysed by sonication. Unbroken cells were removed by centrifugation (5,000 × g, 30min). Membrane fractions were separated from cytosol by ultracentrifugation (100,000 × g, 1h, 4°C) and resuspended in PBS. OMV was separated from culture supernatant by ultracentrifugation (100,000 × g, 2h, 4°C). The pellet (OMV) was resuspended and sonicated briefly in PBS.

**Recombinant OmpA protein production**—Seven OmpA genes were identified in ASF519 genome using Geneious Prime software. Four of them were selected and the gene was amplified by PCR (Invitrogen Fusion High Fidelity PCR kit) using template DNA extracted from ASF mice feces. PCR Primers of each gene are listed in key source table. PCR products were gel purified (Qiagen gel PCR purification kit) and cloned into pET101 vector with C-terminal 6X histidine tag (Invitrogen). The fresh cloning reaction was transformed into TOP10 chemically competent *E. coli* (Invitrogen). Plasmid DNA was extracted (QiaPrep mini kit) from TOP10 culture and sent for Sanger sequencing (Genewiz Inc.). Plasmid with the correct sequence and orientation of each OmpA gene was then transformed into BL21-AI strain (Invitrogen) for expression. Mid-log phased transformed BL21 culture were induced for expression by addition of IPTG (final concentration 0.1mM) and arabinose (0.2%) for 4h at 37°C. Bacterial cells were then pelleted, washed, and lysed by solicitation for 10 s with 30seconds break, for total 3min. Unbroken cells and insoluble lysate were removed by centrifugation. Soluble lysates were purified by Ni-NTA agarose (Qiagen) and eluted with 0.25M Imidazole (300mM NaCl, 50mM phosphate buffer, pH 8.0). Eluate was dialyzed against PBS and quantified by Pierce BCA Protein Assay (Invitrogen). The IL-22 induction activity was assessed by PPC model.

**Intraperitoneal administration of recombinant protein OmpA1**—8-week-old female C57BL/6 mice were purchased from Jackson Labs (Bar Harbor, ME) and maintained on the regular chow diet. Recombinant proteins (40 µg of total protein) were administered intraperitoneally in mice. Serum and ileum were collected at 4h to measure or store for later analysis.

**RNA isolation and qRT-PCR**—Total RNA was extracted from distal ileum tissues (0.5cm) using TRIzol (Invitrogen, Carlsbad, California) according to the manufacturer's protocol. Quantitative RT-PCR was performed using the iScript One-Step RT-PCR Kit with SYBR Green (Bio-Rad, Hercules, California) in a CFX96 apparatus (Bio-Rad, Hercules, California) with the primers listed in key resource table. Differences in transcript levels were quantified by normalization of each amplicon to housekeeping gene 36B4.

**Bacterial Quantification in feces**—Total DNA was isolated from known amounts of feces using QIAamp DNA Stool Mini Kit (Qiagen). DNA was then subjected to quantitative PCR using QuantiNova SYBR Green PCR kit (Qiagen) with primers for 16s rRNA and *OmpA1* of *P. goldsteinii* listed in key resource table to measure DNA copies. Results are normalized by per mg of stool.

**Flow cytometry**—PPCs were incubated with FS-Inu or recombinant protein OmpA for 16h as previously described in Methods. Cell Activation Cocktail with Brefeldin A (Biolegend) was added in PPCs to restimulate cells and to inhibit intracellular protein transport. After 4 h, the activated cells were harvested by centrifugation and washed by PBS. The prepared cells were blocked with 1µg/million cells of 2.4G2 (anti-CD16/anti-32) in 100µL PBS for 15 min at 4°C. This was followed by two washes with PBS to remove any residual blocking antibody. Subsequently, the cells were incubated with conjugated monoclonal antibodies (mABs) including CD8 FITC, Ly6C FITC, B220 FITC, NK1.1

FITC, CD4 APC-eF750, and Ly6G AF700. Cells were then fixed and permeabilized using the Fix/Perm buffer set (eBioscience), followed by intracellular staining with antibodies specific to IL-22 and ROR $\gamma$ t. Multi-parameter analysis was conducted using CytoFlex (Beckman Coulter) and analyzed with FlowJo software (Tree Star).

## QUANTIFICATION AND STATISTICAL ANALYSIS

Data are expressed as means  $\pm$  SEM, except otherwise noted. Statistical significances of results were analyzed by one-tailed unpaired student t-test or one-way analysis of variance (ANOVA) as indicated in Figure legends. n represents number of mice per group. Differences between groups were considered significant at \* $p < 0.05$ , \*\* $p < 0.01$ , \*\*\* $p < 0.001$ , \*\*\*\* $p < 0.0001$ , ns, not significant. Analysis was performed using GraphPad Prism 10.

## Supplementary Material

Refer to Web version on PubMed Central for supplementary material.

## ACKNOWLEDGMENTS

This work was supported by National Institutes of Health grants DK083890 and DK099071 to A.T.G. The graphical abstract was created with [BioRender.com](https://BioRender.com). We thank Dr. Julie Lynn Stoudenmire-Saylor for the valuable advice in recombinant protein purification.

## REFERENCES

- Zenewicz LA (2018). IL-22: There Is a Gap in Our Knowledge. *Immunohorizons* 2, 198–207. 10.4049/immunohorizons.1800006. [PubMed: 31022687]
- Zou J, Chassaing B, Singh V, Pellizzon M, Ricci M, Fythe MD, Kumar MV, and Gewirtz AT (2018). Fiber-Mediated Nourishment of Gut Microbiota Protects against Diet-Induced Obesity by Restoring IL-22-Mediated Colonic Health. *Cell Host Microbe* 23, 41–53.e4. 10.1016/j.chom.2017.11.003. [PubMed: 29276170]
- Klotzkova HB, Kidess E, Nadal AL, and Brugman S (2024). The role of interleukin-22 in mammalian intestinal homeostasis: Friend and foe. *Immun. Inflamm. Dis* 12, e1144. 10.1002/iid3.1144. [PubMed: 38363052]
- Zelante T, Iannitti RG, Cunha C, De Luca A, Giovannini G, Pieraccini G, Zecchi R, D'Angelo C, Massi-Benedetti C, Fallarino F, et al. (2013). Tryptophan catabolites from microbiota engage aryl hydrocarbon receptor and balance mucosal reactivity via interleukin-22. *Immunity* 39, 372–385. 10.1016/j.immuni.2013.08.003. [PubMed: 23973224]
- Kinnebrew MA, Buffie CG, Diehl GE, Zenewicz LA, Leiner I, Hohl TM, Flavell RA, Littman DR, and Pamer EG (2012). Interleukin 23 production by intestinal CD103(+)CD11b(+) dendritic cells in response to bacterial flagellin enhances mucosal innate immune defense. *Immunity* 36, 276–287. 10.1016/j.immuni.2011.12.011. [PubMed: 22306017]
- Yang W, Yu T, Huang X, Bilotta AJ, Xu L, Lu Y, Sun J, Pan F, Zhou J, Zhang W, et al. (2020). Intestinal microbiota-derived short-chain fatty acids regulation of immune cell IL-22 production and gut immunity. *Nat. Commun* 11, 4457. 10.1038/s41467-020-18262-6. [PubMed: 32901017]
- Zindl CL, Lai JF, Lee YK, Maynard CL, Harbour SN, Ouyang W, Chaplin DD, and Weaver CT (2013). IL-22-producing neutrophils contribute to antimicrobial defense and restitution of colonic epithelial integrity during colitis. *Proc. Natl. Acad. Sci. USA* 110, 12768–12773. 10.1073/pnas.1300318110. [PubMed: 23781104]
- Gewirtz AT, Simon PO Jr., Schmitt CK, Taylor LJ, Hagedorn CH, O'Brien AD, Neish AS, and Madara JL (2001). Salmonella typhimurium translocates flagellin across intestinal epithelia,

- inducing a proinflammatory response. *J. Clin. Invest* 107, 99–109. 10.1172/JCI10501. [PubMed: 11134185]
9. Wymore Brand M, Wannemuehler MJ, Phillips GJ, Proctor A, Overstreet AM, Jergens AE, Orcutt RP, and Fox JG (2015). The Altered Schaedler Flora: Continued Applications of a Defined Murine Microbial Community. *ILAR J* 56, 169–178. 10.1093/ilar/ilv012. [PubMed: 26323627]
  10. Macia L, Nanan R, Hosseini-Beheshti E, and Grau GE (2019). Host- and Microbiota-Derived Extracellular Vesicles, Immune Function, and Disease Development. *Int. J. Mol. Sci* 21, 107. 10.3390/ijms21010107. [PubMed: 31877909]
  11. Sakamoto M, and Benno Y (2006). Reclassification of *Bacteroides distasonis*, *Bacteroides goldsteinii* and *Bacteroides merdae* as *Parabacteroides distasonis* gen. nov., comb. nov., *Parabacteroides goldsteinii* comb. nov. and *Parabacteroides merdae* comb. nov. *Int. J. Syst. Evol. Microbiol* 56, 1599–1605. 10.1099/ijs.0.64192-0. [PubMed: 16825636]
  12. Cui Y, Zhang L, Wang X, Yi Y, Shan Y, Liu B, Zhou Y, and Lü X (2022). Roles of intestinal *Parabacteroides* in human health and diseases. *FEMS Microbiol. Lett* 369, fnac072. 10.1093/femsle/fnac072. [PubMed: 35945336]
  13. Koebnik R, Locher KP, and Van Gelder P (2000). Structure and function of bacterial outer membrane proteins: barrels in a nutshell. *Mol. Microbiol* 37, 239–253. 10.1046/j.1365-2958.2000.01983.x. [PubMed: 10931321]
  14. Smith SGJ, Mahon V, Lambert MA, and Fagan RP (2007). A molecular Swiss army knife: OmpA structure, function and expression. *FEMS Microbiol. Lett* 273, 1–11. 10.1111/j.1574-6968.2007.00778.x. [PubMed: 17559395]
  15. Confer AW, and Ayalew S (2013). The OmpA family of proteins: roles in bacterial pathogenesis and immunity. *Vet. Microbiol* 163, 207–222. 10.1016/j.vetmic.2012.08.019. [PubMed: 22986056]
  16. Krishnan S, and Prasadarao NV (2012). Outer membrane protein A and OprF: versatile roles in Gram-negative bacterial infections. *FEBS J* 279, 919–931. 10.1111/j.1742-4658.2012.08482.x. [PubMed: 22240162]
  17. Chalifour A, Jeannin P, Gauchat JF, Blaecke A, Malissard M, N'Guyen T, Thieblemont N, and Delneste Y (2004). Direct bacterial protein PAMP recognition by human NK cells involves TLRs and triggers alpha-defensin production. *Blood* 104, 1778–1783. 10.1182/blood-2003-08-2820. [PubMed: 15166032]
  18. Torres AG, Li Y, Tutt CB, Xin L, Eaves-Pyles T, and Soong L (2006). Outer membrane protein A of *Escherichia coli* O157:H7 stimulates dendritic cell activation. *Infect. Immun* 74, 2676–2685. 10.1128/IAI.74.5.2676-2685.2006. [PubMed: 16622204]
  19. Nie D, Hu Y, Chen Z, Li M, Hou Z, Luo X, Mao X, and Xue X (2020). Outer membrane protein A (OmpA) as a potential therapeutic target for *Acinetobacter baumannii* infection. *J. Biomed. Sci* 27, 26. 10.1186/s12929-020-0617-7. [PubMed: 31954394]
  20. Gophna U, Ideses D, Rosen R, Grundland A, and Ron EZ (2004). OmpA of a septicemic *Escherichia coli* O78—secretion and convergent evolution. *Int. J. Med. Microbiol* 294, 373–381. 10.1016/j.ijmm.2004.08.004. [PubMed: 15595387]
  21. Chassaing B, and Gewirtz AT (2018). Mice harboring pathobiont-free microbiota do not develop intestinal inflammation that normally results from an innate immune deficiency. *PLoS One* 13, e0195310. 10.1371/journal.pone.0195310. [PubMed: 29617463]
  22. Zou J, Ngo VL, Wang Y, Wang Y, and Gewirtz AT (2023). Maternal fiber deprivation alters microbiota in offspring, resulting in low-grade inflammation and predisposition to obesity. *Cell Host Microbe* 31, 45–57.e7. 10.1016/j.chom.2022.10.014. [PubMed: 36493784]
  23. Davies RL, and Quirie M (1996). Intra-specific diversity within *Pasteurella trehalosi* based on variation of capsular polysaccharide, lipopolysaccharide and outer-membrane proteins. *Microbiology (Read.)* 142, 551–560. 10.1099/13500872-142-3-551.

### Highlights

- Fermentable-fiber-enriched diet induces IL-22 in neutrophils and ILC3
- Exposure of Peyer's patch cells to fecal supernatants models IL-22 production *ex vivo*
- OmpA of *Parabacteroides goldsteinii* is enriched by fiber and induces IL-22 expression

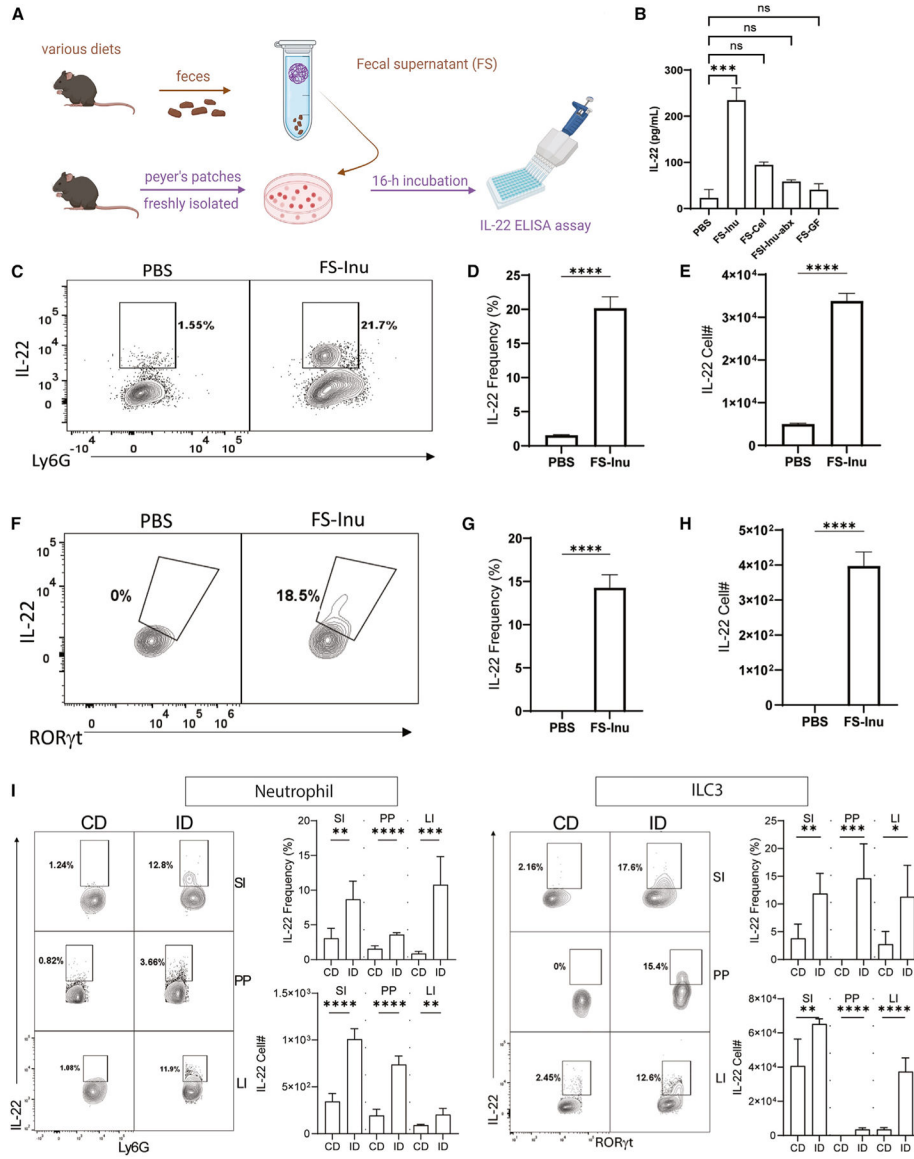


**Figure 1. PPC-based model recapitulates fermentable fiber- and microbiota-dependent induction of IL-22**

(A) Scheme. Feces of C57BL/6 mice fed various diets were collected and resuspended in 100 mg/mL PBS. The fecal supernatant (FS) was added to freshly isolated Peyer’s patch cells (PPCs) at a density of 10<sup>6</sup> cells/200 μL and incubated for 16 h. Culture media were collected to measure IL-22 by ELISA.

(B) IL-22 induction assayed by PPC model in response to FS of conventional mice fed with inulin diet (FS-Inu), cellulose diet (FS-Cel), or inulin diet but with antibiotics in the drinking water (FS-Inu-abx) or FSs of germ-free mice (FS-GF). Data were generated from 18 Peyer’s patches from 4 mice, all of which were pooled, aliquoted 10<sup>6</sup> cells/200 μL, and assayed in duplicate. Data are means ± SEM. \*\*\**p* < 0.001 indicates statistically significant difference from PBS by one-way ANOVA, followed by Dunnett’s multiple comparisons.

(C–H) IL-22<sup>+</sup> neutrophils and ILC3s induced by FS-Inu in PPCs, quantitated by flow cytometry. Data were generated from 29 Peyer’s patches from 4 mice, all of which were

pooled, aliquoted  $10^6$  cells/200  $\mu$ L, and assayed in quadruplicate. (C–E) IL-22<sup>+</sup> neutrophils. (F–H) IL-22<sup>+</sup> ILC3s. The experiment was repeated and similar results attained. Data are means  $\pm$  SEM. \*\*\*\* $p < 0.0001$  indicates statistically significant difference by one-tailed unpaired t test.

(I) Ten-week-old female C57BL/6 mice, raised on grain-based chow, were fed a compositionally defined diet containing 200 g/kg cellulose or inulin, referred to as a cellulose diet (CD) or inulin diet (ID) for 7 days, at which point they were euthanized, and small intestinal lamina propria (SI), Payer's patches (PPs), and large intestinal lamina propria (LI) were isolated. IL-22<sup>+</sup> cells were quantitated by flow cytometry. Data are means  $\pm$  SEM.  $n = 5$ ; \* $p < 0.05$ , \*\* $p < 0.01$ , and \*\*\* $p < 0.001$  indicate statistically significant differences by Student's t test.

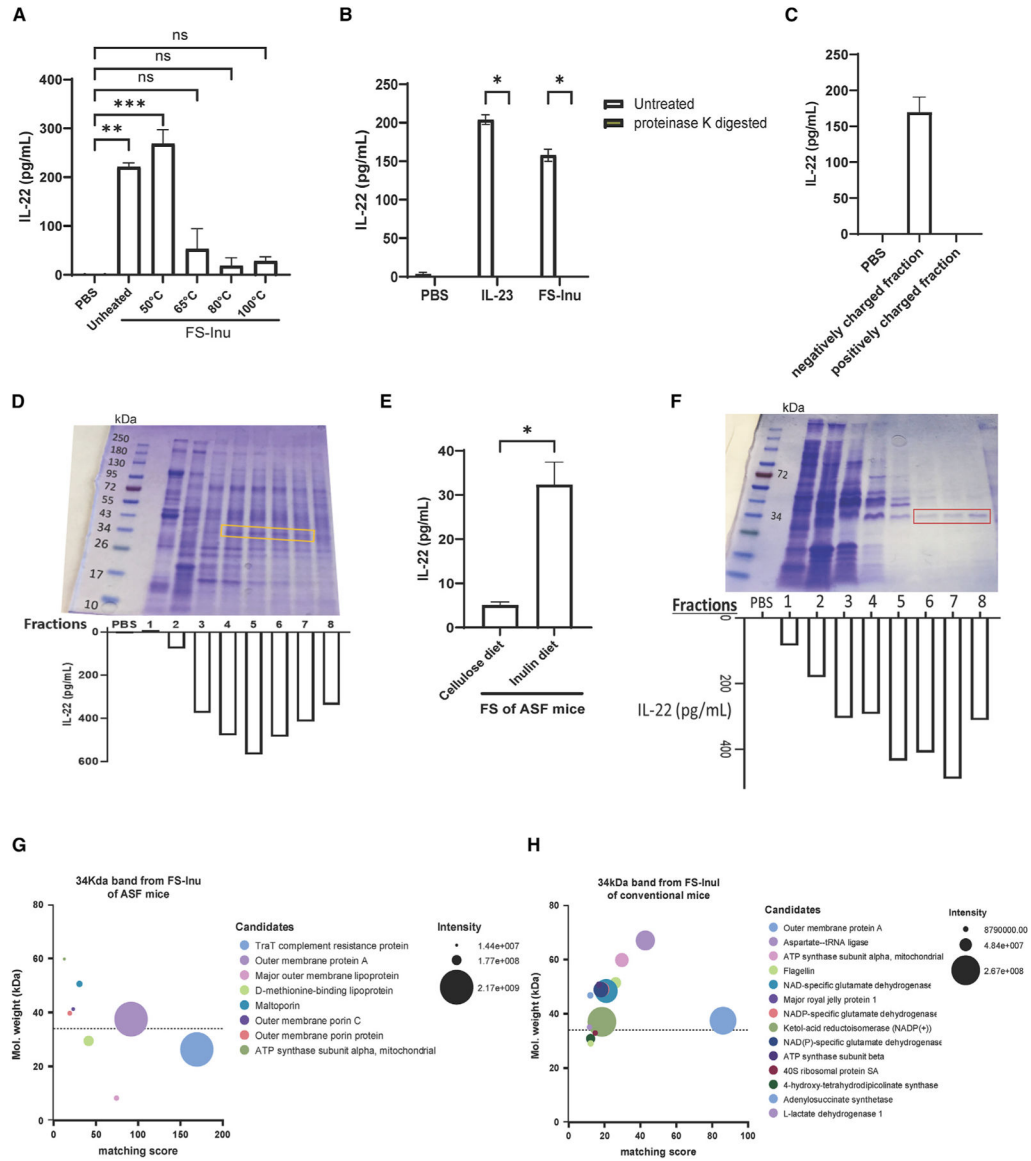


**Figure 2. Characterization of the IL-22-inducing activity of FS-Inu suggests a heat-sensitive protein. Purification and proteomic analysis yields OmpA as a candidate driver of FS-Inu’s IL-22-inducing capacity**

(A) IL-22 production of PPCs in response to FS-Inu heated at 50°C, 65°C, 80°C, or 100°C for 20 min; data were generated from 34 Peyer’s patches from 6 mice, all of which were pooled, aliquoted 10<sup>6</sup> cells/200 μL, and assayed in duplicate. The experiment was repeated and similar results attained. Data are mean(s) ± SEM. \*\**p* < 0.01 and \*\*\**p* < 0.001 indicate statistically significant differences by one-way ANOVA followed by Dunnett’s multiple comparisons to PBS.

(B) IL-22 production of PPCs in response to IL-23 or FS-Inu, treated with proteinase K-linked agarose beads overnight at room temperature with vigorous shaking. Proteinase K beads were removed from the solution by centrifugation. IL-23 was used to confirm the activity of proteinase K. Data were generated from 27 Peyer’s patches from 4 mice, all of which were pooled, aliquoted 10<sup>6</sup> cells/200 μL, and assayed in triplicate. Negative

values were assigned to zero. The experiment was repeated and similar results attained. Data are mean(s)  $\pm$  SEM. \* $p < 0.05$  indicates statistically significant difference by one-tailed unpaired t test.

(C) FS-Inu of conventional mice was fractionated by anion-exchange or cation-exchange spin columns. The IL-22-inducing activity of these fractions was assessed via PPCs. Data were generated from 19 Peyer's patches from 3 mice, all of which were pooled, aliquoted  $10^6$  cells/200  $\mu$ L, and assayed in duplicate. Negative values were assigned to zero. The experiment was repeated and similar results attained. Data are mean(s)  $\pm$  SEM.

(D) FS-Inu of conventional mice was separated by gradient anion-exchange chromatography and visualized by Coomassie blue staining on SDS-PAGE gels. The IL-22 induction activity of each fraction was assessed by a PPC model. A 34 kDa band was identified to be correlated with the IL-22-inducing activity. The activity data were generated from 29 Peyer's patches from 4 mice, all of which were pooled and aliquoted  $10^6$  cells/200  $\mu$ L.

(E) IL-22-inducing activity assessed via PPCs of FSs of ASF mice fed with 20% cellulose diet or 20% inulin diet. Data were generated from 13 Peyer's patches from 2 mice, all of which were pooled, aliquoted  $10^6$  cells/200  $\mu$ L, and assayed in duplicate. The experiment was repeated and similar results attained. Data are mean(s)  $\pm$  SEM. \* $p < 0.05$  indicates statistically significant difference by one-tailed unpaired t test.

(F) FS-Inu of ASF mice's counterpart of (D). The activity data were generated from 18 Peyer's patches from 3 mice, all of which were pooled and aliquoted  $10^6$  cells/200  $\mu$ L.

(G and H) The 34 kDa bands from (F) and (D) respectively were excised from the gel and analyzed by mass spectrometry. Matching score, molecular weight, and intensity of each protein candidate generated by the proteomic analysis are shown in the bubble plot.

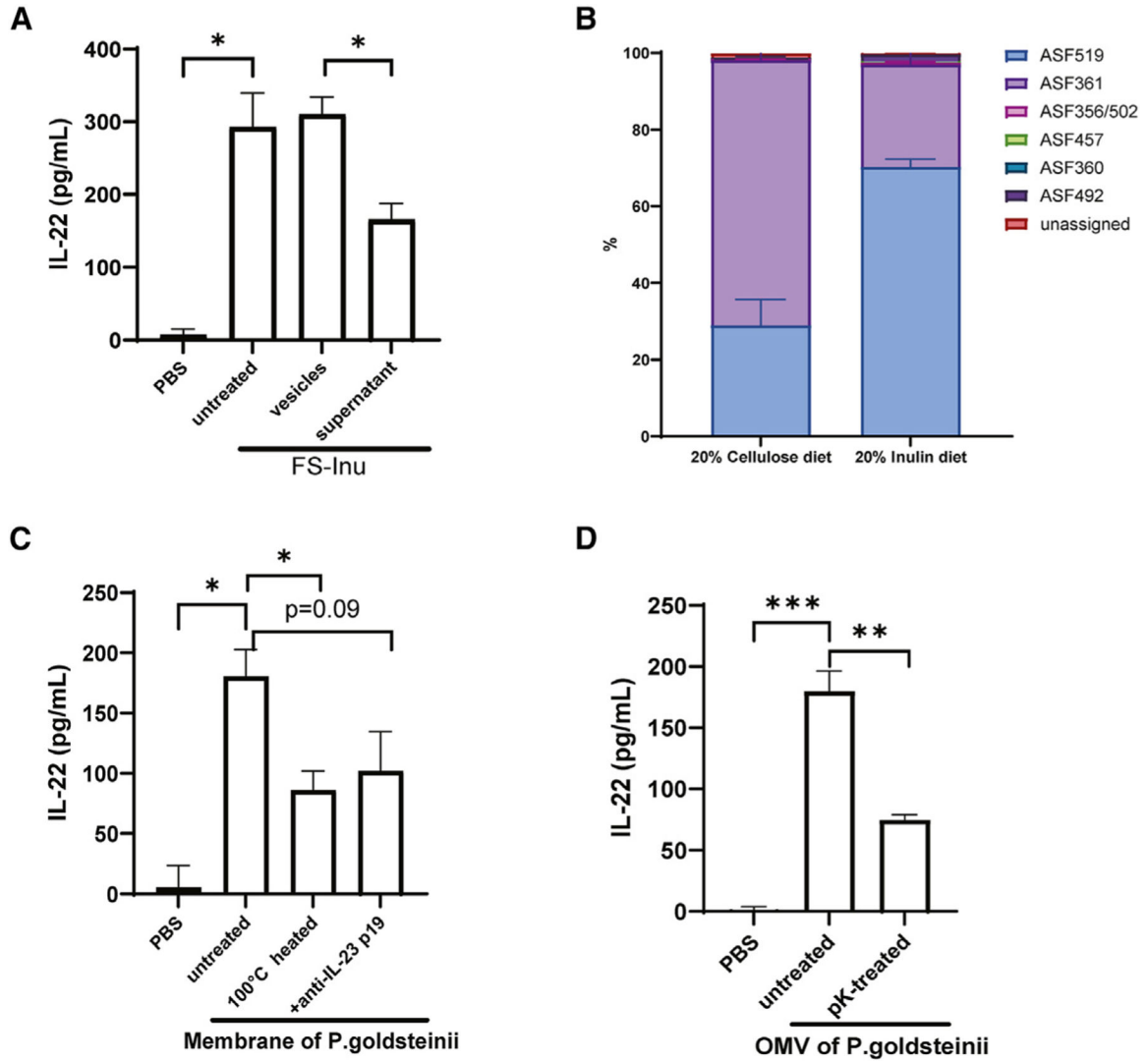


**Figure 3. Membrane and OMVs of *Parabacteroides goldsteinii* strain ASF519 induce IL-22 in PPCs**

(A) Vesicles were separated from FS-Inu by ultracentrifugation. Untreated, vesicles and the supernatant after vesicle removal of FS-Inu containing the same amount of total protein (15 µg) were assayed for IL-22-inducing activity in PPCs. Data were generated from 22 Peyer’s patches from 4 mice, all of which were pooled, aliquoted 10<sup>6</sup> cells/200 µL, and assayed in duplicate. The experiment was repeated and similar results attained.

(B) Fecal microbiota composition via 16S rRNA gene sequencing of ASF mice fed with either 20% cellulose diet or 20% inulin diet suggests *P. goldsteinii* strain ASF519 was greatly enriched by inulin diet. *n* = 2 ASF mice per group.

(C) Membranes of pure culture *P. goldsteinii* strain ASF519 untreated, supplemented with anti-IL-23 p19 neutralizing antibody, or heated (100°C for 20 min) were assayed for IL-22-inducing activity by PPC model. These samples were assayed together with Figure S2B and shared the data of the PBS group. Data were generated from 35 Peyer’s patches from 6 mice, all of which were pooled, aliquoted 10<sup>6</sup> cells/200 µL, and assayed in duplicate. The experiment was repeated and similar results attained.

(D) OMV of *P. goldsteinii* strain ASF519 was treated with or without proteinase K (pK)-linked agarose beads overnight at room temperature with vigorous shaking. Proteinase K beads were removed from the solution by centrifugation. IL-22 inducing activity was assayed by a PPC model. Data were generated from 40 Peyer's patches from 5 mice, all of which were pooled, aliquoted  $10^6$  cells/200  $\mu$ L, and assayed in duplicate. Data are means  $\pm$  SEM. \* $p < 0.05$ , \*\* $p < 0.01$ , and \*\*\* $p < 0.001$  indicate statistically significant differences by one-tailed unpaired t test.

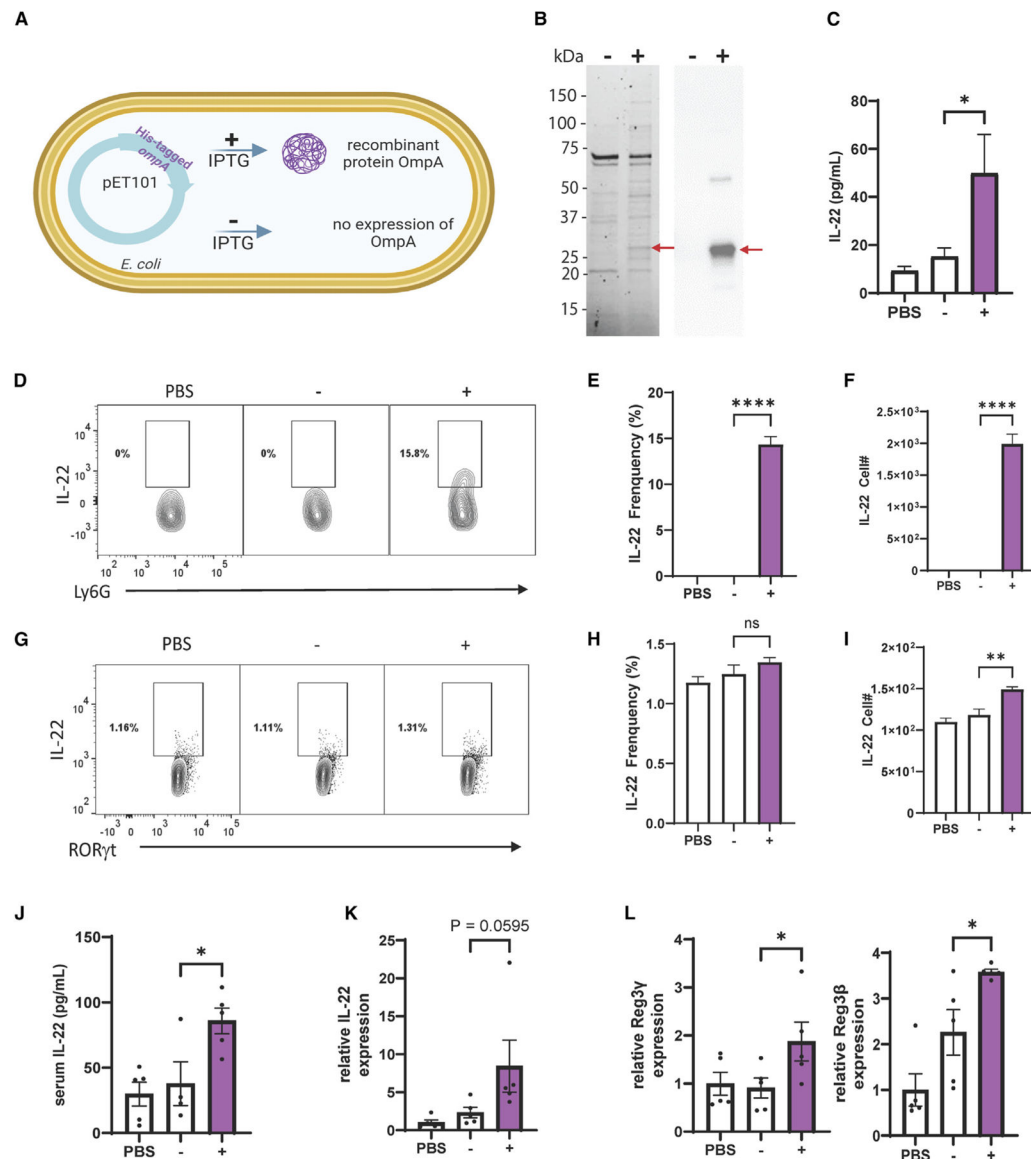


**Figure 4. Recombinant protein OmpA1 of *Parabacteroides goldsteinii* induces IL-22 in PPCs and *in vivo***

(A) Scheme of IPTG-induced recombinant protein OmpA1 production in *E. coli BL21* strain.

(B) Total proteins of recombinant protein OmpA1 from IPTG-induced culture (denoted as “+”) and expression control from IPTG-uninduced counterpart (denoted as “-”) were visualized on stain-free SDS-PAGE (left) and blotted for His tag (right) at targeted molecular weight of 28 kDa.

(C) IL-22-inducing activity of OmpA1 and its expression control assayed by PPC model (5  $\mu\text{g/mL}$  of total proteins). Data were generated from 23 Peyer’s patches from 3 mice, all of which were pooled, aliquoted  $10^6$  cells/200  $\mu\text{L}$ , and assayed in quadruplicate. Data are mean  $\pm$  SEM. \* $p < 0.05$  indicates statistically significant differences by one-tailed unpaired t test.

(D–I) IL-22<sup>+</sup> neutrophils and ILC3s are induced by recombinant OmpA1 in PPCs, quantitated by flow cytometry. Data were generated from 40 Peyer’s patches from 5 mice,

all of which were pooled, aliquoted  $10^6$  cells/200  $\mu$ L, and assayed in quintuplicate. Data are mean  $\pm$  SEM. \*\* $p < 0.01$ , and \*\*\*\* $p < 0.0001$  indicate statistically significant differences by one-tailed unpaired t test.

(D–I) IL-22<sup>+</sup> neutrophils in PPCs (D–F) and IL-22<sup>+</sup> ILC3s in PPCs. (G–I).

(J–L) Mice were intraperitoneally administrated OmpA1 (40  $\mu$ g of total proteins per mouse,  $n = 5$  mice per group). Serum and ileum were collected 4 h later. Serum IL-22 was assayed by ELISA (J). RNA was isolated from distal ileum (0.5 cm). mRNA encoding IL-22 (K), Reg3 $\gamma$  (L, left), and Reg3 $\beta$  (L, right) were quantitated by real-time qPCR and normalized to 36B4. Data are represented as a fold change of the PBS group. Data are means  $\pm$  SEM. \* $p < 0.05$  indicates statistically significant differences by one-tailed unpaired t test.

## KEY RESOURCES TABLE

REAGENT or RESOURCE	SOURCE	IDENTIFIER
<b>Antibodies</b>		
Anti-His	Biolegend	Cat# 652503; RRID: AB_2734520
IL-23 p19 Monoclonal Antibody (G23-8)	eBioscience	Cat# 16-7232-81; RRID: AB_469240
IL-22 Monoclonal Antibody (1H8PWSR)	eBioscience	Cat# 12-7221-82; RRID: AB_10597428
ROR gamma (t) Monoclonal Antibody (B2D)	eBioscience	Cat# 17-6981-82; RRID: AB_2573254
CD4 Monoclonal Antibody (RM4-5), APC	eBioscience	Cat# 17-0042-82; RRID: AB_469323
LIVE/DEAD™ Fixable Aqua Dead Cell Stain Kit, for 405 nm excitation	ThermoFisher Scientific	Cat# L34966; RRID: N/A
Ly-6G Monoclonal Antibody (1A8-Ly6g), Alexa Fluor™ 700	eBioscience	Cat# 56-9668-82; RRID: AB_2802355
CD8 alpha Monoclonal Antibody (53-6.7), FITC	Invitrogen	Cat# MA1-10303; RRID: AB_11153636
CD45R (B220) Monoclonal Antibody (HIS24), FITC	eBioscience	Cat# 11-0460-82; RRID: AB_465075
FITC anti-mouse Ly-6C Antibody	BioLegend	Cat# 128006; RRID: AB_1186134
FITC anti-mouse NK-1.1 Antibody	BioLegend	Cat# 108706; RRID: AB_313393
<b>Bacterial and virus strains</b>		
<i>Parabacteroides goldsteinii</i> strain ASF519	lab	N/A
One Shot™ TOP10 Chemically Competent <i>E. coli</i>	Invitrogen	Cat# C404003
One Shot™ BL21-AI™ Chemically Competent <i>E. coli</i>	Invitrogen	Cat# C607003
Salmonella Typhimurium str. LT2	lab	N/A
Altered Schaedler Flora	ASF Taconic Inc.	N/A
<b>Chemicals, peptides, and recombinant proteins</b>		
Lipopolysaccharides	Sigma-Aldrich	Cat# I2887
Ampicillin	Sigma-Aldrich	Cat# A9518-100G
Neomycin	Sigma-Aldrich	Cat# N1876-100G
Vancomycin	Sigma-Aldrich	Cat# V2002-250MG
Metronidazole	Sigma-Aldrich	Cat# M1547-25G
Sodium butyrate	Sigma-Aldrich	Cat# 303410-100G
IPTG	Invitrogen	Cat# AM9464
L(+)-Arabinose	Thermo Scientific	Cat# 365180250
Imidazole	Sigma-Aldrich	Cat# I2399-100G
N-Formyl-Met-Leu-Phe	Sigma-Aldrich	Cat# F3506-10MG

REAGENT or RESOURCE	SOURCE	IDENTIFIER
Proteinase K–Agarose	Sigma-Aldrich	Cat# P9290-10UN
Carbenicillin disodium salt	Sigma-Aldrich	Cat# C3416-250MG
Cell Activation Cocktail (with Brefeldin A)	BioLegend	Cat # 423303
eBioscience™ Foxp3/Transcription Factor Staining Buffer Set	ThermoFisher Scientific	Cat# 00-5523-00
eBioscience™ Permeabilization Buffer (10X)	eBioscience	Cat# 00-8333-56
Percol Plus	Cytiva	Cat#17544501
Type IV collagenase	Sigma-Aldrich	Cat#C5138-5G
DNAse I	Sigma-Aldrich	Cat#10104159001
Critical commercial assays		
QIAamp DNA Stool Mini Kit	Qiagen	Cat# 51504
One-Step RT–PCR Kit with SYBR Green	Bio-Rad	Cat# 172-5151
IL-22 ELISA Kit	R&D Systems	Cat# DY582
QuantiNova SYBR Green PCR Kit	Qiagen	Cat# 208052
Pierce™ Rapid Gold BCA Protein Assay Kit	Thermo Scientific	Cat# A53225
Mouse/Rat IL-22 Quantikine ELISA Kit	R&D Systems	Cat# M2200
Deposited data		
16S rRNA sequence	NCBI Sequence Read Archive	SRA: PRJNA1089129
Processed proteomics data	Georgia State University institutional repository	GSU: <a href="https://doi.org/10.57709/VK8T-YA18">https://doi.org/10.57709/VK8T-YA18</a>
Experimental models: Organisms/strains		
Mice: C57BL/6	Jackson Laboratory	Cat# 000664
Oligonucleotides		
16S rRNA sequencing primers: 5'-TCGTCCGCGAGCGTCAGATGTGTATAAGAGACAGCCTACGGGNGGCWGCAG-3';	Invitrogen	N/A
16S rRNA sequencing primers: 5'-GTCTCGTGGGCTCGGAGATGTGTATAAGAGACAGGACTACHVGGGTATCTAATCC-3'.	Invitrogen	N/A
36B4: 5'-TCCAGGCTTTGGGCATCA-3'	Invitrogen	N/A
36B4:5'-CTTTATTCAGCTGCACATCACTCAGA-3'	Invitrogen	N/A
IL-22: 5'-GTGCTCAACTTCACCCTGGA-3'	Invitrogen	N/A
IL-22: 5'- TGGATGTTCTGGTCGTCACC-3'	Invitrogen	N/A
ompA1: 5'-ACAATACCGGTAAGGAACAGCC-3'	Invitrogen	N/A
ompA1: 5'-TGTATTACCGCCAATGCACCAAT-3'	Invitrogen	N/A
ompA1 cloning primer: 5'-CACCATGAAACATTTAAACTATTATCAG-3'	Invitrogen	N/A
ompA1 cloning primer: 5'-TTTCAATGTCCCTGTTGAG-3'	Invitrogen	N/A
ompA3 cloning primer: 5'-CACCATGAATAAGAAGATTACTCCC-3'	Invitrogen	N/A

REAGENT or RESOURCE	SOURCE	IDENTIFIER
ompA3 cloning primer: 5'-GAACAGGTTATAGTTTGTCTGAG-3'	Invitrogen	N/A
ompA4 cloning primer: 5'- CACCATGAAAAAGTATTTGTTTATTATGG-3'	Invitrogen	N/A
ompA4 cloning primer: 5'-TTGTTCTACGTAAAGAATCACGG-3'	Invitrogen	N/A
ompA5 cloning primer: 5'- CACCATGAAGACTAAAGTATTACTTTTA -3'	Invitrogen	N/A
ompA5 cloning primer: 5'-ATTATTAGCAGACATGATAACAACAC-3'	Invitrogen	N/A
Salmonella Typhimurium str. LT2 ompA cloning primer: 5'- CACCATGAAAAAGACAGCTATCG-3'	Invitrogen	N/A
Salmonella Typhimurium str. LT2 ompA cloning primer: 5'-AGCCTGCGGCTGAGTTA-3'	Invitrogen	N/A
Reg3 $\gamma$ : 5'-CGTGCCTATGGCTCCTATTGCT- 3'	Invitrogen	N/A
Reg3 $\gamma$ : 5'- TTCAGCGCCACTGAGCACAGAC- 3'	Invitrogen	N/A
Reg3 $\beta$ : 5'-CTCCTGCCTGATGCTCTTAT-3'	Invitrogen	N/A
Reg3 $\beta$ : 5'-TTGTTACTCCATCCCATCC-3'	Invitrogen	N/A
P.goldsteinii 16s primer: 5'- GCAGCAGATGTAGCAATACA-3'	Invitrogen	N/A
P.goldsteinii 16s primer: 5'- TTAACAAATATTTCCATGTGGAAC-3'	Invitrogen	N/A
Software and algorithms		
GraphPad Prism	GraphPad Software	N/A
Geneious Prime	GraphPad Software	N/A
FlowJo	BD	<a href="https://www.flowjo.com/">https://www.flowjo.com/</a>
Other		
Champion™ pET101 Directional TOPO™ Expression Kit	Invitrogen	Cat# K10101
Inulin-enriched diet	Research Diets	Cat #D13081108
Cellulose-enriched diet	Research Diets	Cat #D13081109